Article

J. Mex. Chem. Soc. **2024**, *68*(4)
Special Issue

ISSN-e 2594-0317

Entropic Uncertainty Relations and Mutual Information Correlation Sums in Two-level Superposition States of Coupled Oscillators

Saúl J. C. Salazar[1], Humberto G. Laguna[1], Angel Garcia-Chung[1,2,3], Robin P. Sagar[1]

[1]Departamento de Química, Universidad Autónoma Metropolitana, Avenida Ferrocarril San Rafael Atlixco No. 186, Leyes de Reforma 1a Sección, Iztapalapa, 09310, Ciudad de México, México.
[2]Max Planck Institute for Mathematics in the Sciences, Leipzig, Germany.
[3]Tecnológico de Monterrey, Escuela de Ingeniería y Ciencias, Estado de México 52926, México.

***Corresponding author:** Humberto G. Laguna, email: hlaguna@izt.uam.mx

Received May 1st, 2024; Accepted July 3th, 2024.

DOI: http://dx.doi.org/10.29356/jmcs.v68i4.2265

Abstract. The effects of quantum interferences and interaction strength on the entropic uncertainty relations, and on mutual information correlation sums, are examined in two-level superposition states of two coupled oscillators. The presence of quantum interferences results in a movement of the entropy sums toward the uncertainty relation bound, for both attractive and repulsive interaction potentials. On the other hand, these interferences suppress the statistical correlations in the presence of an attractive potential, while the correlations increase for a repulsive one. In general, stronger interactions between particles move the entropy sums away from bound, with the result that the systems possess larger statistical correlations. However, there are superposition and attractive interaction regimes, where the entropy sum of an interacting system can actually lie closer to the bound, in comparison to the corresponding non-interacting one. In these cases, the statistical correlations between particles is lesser for the interacting systems, as compared to the non-interacting ones. These effects are not observed when repulsive potentials are present. Here, the non-interacting systems lower-bound both the entropy sums and correlation measures. These results offer insights into the nature of superposition or quantum interference effects in interacting quantum systems, and the behavior in terms of the entropic uncertainty relations, statistical correlations and interaction strength.
Keywords: Entropic uncertainty relations; mutual information; information theory; momentum space; coupled oscillators.

Resumen. Se examinan los efectos que las interferencias cuánticas y la magnitud de la interacción tienen sobre las relaciones de incertidumbre entrópicas, así como sobre las sumas correlaciones me didas a través de la información mutua, en estados de superposición de dos niveles de dos osciladores acoplados. La presencia de interferencias cuánticas da como resultado un movimiento de las sumas entrópicas hacia la cota de la relación de incertidumbre, tanto para potenciales de interacción atractivos como repulsivos. Por otra parte, en presencia de un potencial atractivo, estas interferencias suprimen las correlaciones estadísticas, mientras que las correlaciones aumentan en presencia de uno repulsivo. En general, con interacciones más fuertes entre partículas, las sumas de entrópicas se alejan de la cota, dando como resultado mayores correlaciones estadísticas en los sistemas. Sin embargo, existen regímenes de superposición e interacción atractiva, en los cuales la suma entrópica de un sistema interactuante puede estar más cerca de la cota, en comparación con el sistema no interactuante correspondiente. En estos casos, las correlaciones estadísticas entre partículas son menores para los sistemas interactúantes que para los no interactuantes. Estos efectos no se observan en los potenciales repulsivos. En este caso, los sistemas no interactuantes establecen límites inferiores tanto para las sumas entrópicas como para las medidas de correlación. Estos resultados dan información sobre la naturaleza de los efectos de superposición o interferencia cuántica en

J. Mex. Chem. Soc. **2024**, *68*(4)
Special Issue

ISSN-e 2594-0317

sistemas cuánticos interactuantes, y su comportamiento en términos de relaciones de incertidumbre entrópica, correlaciones estadísticas y fuerza de interacción.
Palabras clave: Relaciones de incertidumbre entrópica; information mutua; teoría de la información; espacio de momento; osciladores acoplados.

Introduction

The Heisenberg uncertainty principle is a principal element of quantum mechanics. Much discussion has centered around its analysis and interpretation, and of the limits it provides about the behaviour of quantum systems. In recent decades, there has been a migration away from the textbook Kennard-Robertson formulation in terms of standard deviations [1], to ones in terms of Shannon information entropies, or indeed of other entropies. Developments in femtosecond spectroscopy allow one to examine chemistry at the uncertainty limit [2]. To celebrate the fiftieth anniversary of UAMI, we will first present a brief review of what has been accomplished with information theory in previous years, before moving on to discuss the particular problem.

The Shannon entropic uncertainty relation [3–6] is given as

$$S_{(N\cdot D)_x} + S_{(N\cdot D)_p} > \ln(\pi e\hbar)^{N\cdot D} \tag{1}$$

where *D* is the dimension of the system and N is the number of particles. The focus of this work will be to consider D = 1 and one and two particle systems, for which we will employ the notation of S_t and S_T, to indicate the respective entropy sums in the equation above. The Shannon entropies in position (*x*) and in momentum (*p*) space are defined in terms of the one-particle wave functions or densities as

$$\begin{aligned} S_x = S_{1_x} &= -\int |\Psi(x)|^2 \ln|\Psi(x)|^2 \, dx, \\ S_p = S_{1_p} &= -\int |\Phi(p)|^2 \ln|\Phi(p)|^2 \, dp. \end{aligned} \tag{2}$$

The integration limits depend on the particular coordinate system that is used to represent the system. The wave function, Ψ(*x*), in the position representation, is connected to Φ(*p*), the one in the momentum representation, by the Dirac-Fourier transform. All densities used in this work are normalized to unity and the integration limits are (-∞, +∞).

One-particle Shannon entropies can also be obtained from a *N*-particle wave function or density, by first integrating over the $N-1$ particles to obtain one-particle reduced densities,

$$\begin{aligned} \rho(x) &= \int |\Psi(x, x_2, \cdots, x_N)|^2 dx_2 \ldots dx_N, \\ \pi(p) &= \int |\Phi(p, p_2, \cdots, p_N)|^2 dp_2 \ldots dp_N, \end{aligned} \tag{3}$$

Shannon entropies for these reduced densities are obtained by replacing $|\Psi(x)|^2$ and $|\Phi(p)|^2$ by the reduced densities, $\rho(x)$ and $\pi(p)$, in Eq. (2). The Shannon entropies in each representation are measures of the (de)localization in the underlying distributions. Their values increase as the distributions delocalize and decrease when they localize. In fact, the Shannon entropy of a continuous distribution can be negative-valued, in contrast to a discrete one which is lower-bounded by zero. It should not be surprising that these measures have attracted attention in quantum chemistry, where questions of electron localization and delocalization are prevalent concepts. These are global measures of (de)localization in the system, in contrast to local ones which aim to locate regions within the system where electrons are localized. In a more general context, localization is

J. Mex. Chem. Soc. **2024**, *68*(4)
Special Issue

ISSN-e 2594-0317

associated with phenomena resulting from wave interference, within the quantum mechanical framework. There has been keen interest in understanding the behaviour of the Shannon entropy sum in a variety of different quantum systems [6–24]. In quantum chemistry, one of the first works involved a study of the behaviour in neutral and charged atoms, as well as in the harmonic oscillator, in ground and excited states [7]. The idea put forth at this time was that the entropy sum serves as a measure of wave function quality and could be thus employed in quantum chemistry. The Shannon entropy, in the context of atomic systems, is a functional of the one-electron density, so it should also not be surprising that this work originated from a renowned density functional laboratory. Later, it was proposed that the entropy sum could be used as a correlation measure in atomic systems [10]. These ideas propelled interest into the study of molecular systems [25,26]. It was also noted that the position space Shannon entropy emerges naturally from the logarithmic mean excitation energy within the local plasma approximation, used in stopping power measurements and experiments [27].

The entropy sum is also of interest in quantum chemistry, since it combines perspectives from both the position and momentum space representations. While the position or coordinate space representation is prevalent in quantum chemistry, there has also been efforts to develop a momentum space quantum chemistry [28]. Other avenues of interest include study of the time dependent behaviour of S_t, which has been analysed in simple systems [29,30]. There has also been interest in the application of these measures to study Bose-Einstein condensates [21,22]. The relation of the entropy sum with the entropies of the marginals of the Wigner phase-space distribution has also been documented [31]. Shannon entropies of phase-space quantum distributions have been considered [31,32].

Recently, there has been considerable activity in the examination of the entropy sum in confined quantum systems, to examine the influence of physical barriers, potentials, and static and dynamic external fields [33–44]. To date, these studies have been limited to few-particle systems, however one can expect that larger systems will be addressed in the near future. Several groups in both the chemistry and physics departments of UAM-Iztapalapa are actively engaged in using Shannon measures to furthering the understanding of behaviour in confined quantum systems.

One can also consider the Shannon entropies of the pair densities in position and in momentum space, for two or more particle systems. To date, these entropies have not seen a widespread interest, as compared to the one-particle ones. Pair densities represent the probabilities of finding one particle with a particular position (momentum), and the other particle with another position (momentum). Thus, questions of particle interaction, and indeed chemical bonding in molecular systems, should be naturally encoded into these quantities. There is active research into the development of a pair density functional theory [45–47].

The Shannon pair entropy components and their sum [in Eq. (2)] have been examined in atomic systems [48–50] and in two- and three-particle coupled oscillators [51,52]. These entropies can be defined in terms of two-particle wave functions as ($S_\Gamma = S_{2_x}, S_\Pi = S_{2_p}$)

$$S_\Gamma = -\int |\Psi(x_1, x_2)|^2 \ln |\Psi(x_1, x_2)|^2 \, dx_1 dx_2,$$
$$S_\Pi = -\int |\Phi(p_1, p_2)|^2 \ln |\Phi(p_1, p_2)|^2 \, dp_1 dp_2. \tag{4}$$

The S_T results from summation of S_Γ and S_Π. One can also calculate Shannon pair entropies from reduced densities of N-particle systems which have been reduced by integrating over $N-2$ particles,

$$\Gamma(x_1, x_2) = \int |\Psi(x_1, x_2, \cdots, x_N)|^2 dx_3 \cdots dx_N,$$
$$\Pi(p_1, p_2) = \int |\Phi(p_1, p_2, \cdots, p_N)|^2 dp_3 \cdots dp_N. \tag{5}$$

For the two-particle systems in this work, there is no reduction to get the pair density since it is the squared norm of the two-particle wave function. It is hoped that the coming years will bear witness to an increasing interest in pair density information measures, especially in molecular systems.

J. Mex. Chem. Soc. **2024**, *68*(4)
Special Issue

ISSN-e 2594-0317

The electron correlation problem is one that is particularly relevant in quantum chemistry, and results from the fact that there is no exact solution to the Schrödinger equation when electrons interact through repulsive Coulomb potentials. Indeed, quantum chemistry can be conceived as a field devoted to the development of methods to obtain approximate solutions of varying accuracies. Hence, there was a need for a measure to adequately capture the inclusion or exclusion of interaction effects in the wave function. The correlation energy was introduced [53] as the difference between the exact non-relativistic energy and the Hartree-Fock energy of the particular system. This quantity was thus used as a measure of evaluating the approximate wave function. It is important to emphasize here that this evaluation is not directly based on the wave function but rather on its corresponding energy. Furthermore, the Fermi correlation due to the antisymmetry of the wave function, is not included, since it is presumably subtracted out in the Hartree-Fock reference.

On the other hand, other avenues of defining correlation through statistical correlation measures have a long history [54–56]. This seems a natural evolution due to the Born interpretation of the wave function as a probability density. Hence, correlation is measured here not from the energy perspective, but rather from the wave function characteristics, in terms of the associated probability distribution. The statistical correlation coefficient from statistics was introduced as one such measure [55,56]. It captures linear relations between variables by examining differences between (linear) expectation values of the pair densities and those of the one-particle densities. One advantage is that these measures do not depend on the selection of a particular external reference such as Hartree-Fock. However, they include all correlation effects, including those from the interactions and also the symmetry of the wave function.

Pair mutual information is another statistical correlation measure, which is capable of capturing the non-linear correlations. It has been utilized in many distinct areas, both in its discrete and continuous forms [52, 57–65]. It is defined in position and in momentum space as

$$I_x = \int \Gamma(x_1, x_2) \ln \left[\frac{\Gamma(x_1, x_2)}{\rho(x_1)\rho(x_2)} \right] dx_1 dx_2 = 2S_\rho - S_\Gamma \geq 0 \tag{6}$$

$$I_p = \int \Pi(p, p_2) \ln \left[\frac{\Pi(p_1, p_2)}{\pi(p_1)\pi(p_2)} \right] dp_1 dp_2 = 2S_\pi - S_\Pi \geq 0 \tag{7}$$

In this work, the marginals of the pair densities in the denominator of the logarithmic arguments are the one-particle reduced densities defined in Eq. (3) with $N = 2$. Note that the two marginals are equal, due to particle indistinguishability of the quantum mechanical density. In the general case, these are not necessarily equal. These measures have been examined in the ground and excited states of atomic systems and coupled oscillators [51, 52, 66]. The sum of the position and momentum space mutual information will be given as

$$I_t = I_x + I_p = 2S_t - S_T \geq 0. \tag{8}$$

I_t quantifies the correlation, by taking the weighted difference between the one- and two-variable entropy sums. Statistical correlation measures provide a means to directly examine, interpret and relate behaviour, with that of the interactions that are present in a particular system. This is distinct from the previous vision of defining a correlation measure for the purpose of classifying the goodness of an approximate wave function. Quantum chemistry calculations yield approximate wave functions and densities. Thus, there is always the question if interpretation of phenomena from a particular calculation is valid, or a product of the limitations of the particular method that is used. In these instances, model systems which yield exact wave functions and densities, can offer a guide to illuminate the path forward. One such system consists of two oscillators that are coupled by a harmonic two-body potential [67] and has been used in density functional theory [68–74].

J. Mex. Chem. Soc. **2024**, *68*(4)
Special Issue

ISSN-e 2594-0317

The model: Two-particle coupled oscillators

The Hamiltonian of two coupled oscillators in canonical coordinates in position space, considering atomic units ($m = \hbar = 1$) is

$$H = -\frac{1}{2}\left(\frac{\partial^2}{\partial x_1^2} + \frac{\partial^2}{\partial x_2^2}\right) + \frac{1}{2}\omega^2(x_1^2 + x_2^2) \pm \lambda^2(x_1 - x_2)^2, \tag{9}$$

where ω is the natural frequency of the oscillators and λ is the intensity of the interaction potential, with the positive sign for the attractive case and the negative sign for the repulsive case. The value of λ is bounded for the repulsive case by $\lambda < \omega/\sqrt{2}$ in order to obtain a bound state.

The canonical coordinates in position space (x_1, x_2) can be transformed into Jacobi coordinates (R, r), thus the eigenfunction is separable in the new coordinates, and can be written as a product of two eigenfunctions

$$\Psi(x_1, x_2) = \psi_{n_R}(R)\psi_{n_r}(r) \tag{10}$$

with

$$\psi_{n_R}(R) = \left(\frac{\alpha_1^{\frac{1}{4}}}{2^{n_R}\, n_R!\, \pi^{\frac{1}{2}}}\right)^{\frac{1}{2}} e^{-\frac{1}{2}\sqrt{\alpha_1}R^2}\, H_{n_R}\left(\alpha_1^{\frac{1}{4}}\, R\right), \qquad n_R = 0,1, \ldots \tag{11}$$

$$\psi_{n_r}(r) = \left(\frac{\alpha_2^{\frac{1}{4}}}{2^{n_r}\, n_r!\, \pi^{\frac{1}{2}}}\right)^{\frac{1}{2}} e^{-\frac{1}{2}\sqrt{\alpha_2}r^2}\, H_{n_r}\left(\alpha_2^{\frac{1}{4}}\, r\right), \qquad n_r = 0,1, \ldots \tag{12}$$

Here $\alpha_1 = \omega^2$, $\alpha_2 = \omega^2 \pm 2\lambda^2$, $H_n(x)$ is an $n^{th}-$ order Hermite polynomial and n_R and n_r are the quantum numbers labelling the center of mass (R) and relative (r) coordinates. The symmetry of the wave function is controlled by the value of the n_r quantum number. Symmetric wave functions have even-valued n_r, while in antisymmetric ones they are odd-valued. For example, the $|n_R\, n_r\rangle = |\,00\,\rangle$ state is symmetric while the $|01\rangle$ one is antisymmetric.

The wave function in momentum space, can be obtained by applying the Fourier transform to the wave function in position space to get

$$\Phi(p_1, p_2) = \phi_{n_R}(P)\phi_{n_r}(p), \tag{13}$$

with

$$\phi_{n_R}(P) = (-i)^{n_R}\left(\frac{1}{2^{n_R}\, n_R!\; \alpha_1^{\frac{1}{4}}\, \pi^{\frac{1}{2}}}\right)^{\frac{1}{2}} e^{-\frac{P^2}{2\sqrt{\alpha_1}}}\, H_{n_R}\left(\frac{P}{\alpha_1^{\frac{1}{4}}}\right), \qquad n_R = 0,1, \ldots \tag{14}$$

J. Mex. Chem. Soc. **2024**, *68*(4)
Special Issue

ISSN-e 2594-0317

$$\phi_{n_r}(p) = (-i)^{n_r}\left(\frac{1}{2^{n_r}\, n_r!\; \alpha_2^{\frac{1}{4}}\, \pi^{\frac{1}{2}}}\right)^{\frac{1}{2}} e^{-\frac{p^2}{2\sqrt{\alpha_2}}} H_{n_r}\left(\frac{p}{\alpha_2^{\frac{1}{4}}}\right), \quad n_r = 0,1,\ldots \tag{15}$$

The pair densities in each representation are obtained as the squared norm of the respective wave function, while the reduced densities or marginals are obtained by integration over one of the original variables.

In the non-interacting limit ($\lambda = 0$), the wave function can be expressed as symmetric or antisymmetric products of orbitals, where each orbital is the harmonic oscillator solution for a particular quantum number. Taking the non-interacting state with quantum numbers (0,1) in position space as one example yields,

$$\Psi_{0,1} = \psi_0(x_1)\psi_1(x_2) - \psi_1(x_1)\psi_0(x_2), \tag{16}$$

where the orbitals here are given as

$$\psi_n(x) = \frac{1}{\sqrt{2^n n!}}\left(\frac{\omega}{\pi}\right)^{\frac{1}{4}} e^{-\frac{\omega x^2}{2}} H_n\left(\sqrt{\omega}\, x\right), \quad -\infty \le x \le \infty, \quad n = 0,1,\ldots. \tag{17}$$

The momentum space wave function can be defined in an analogous manner with orbitals

$$\phi_n(p) = \frac{(-i)^n}{\sqrt{2^n n!}}\left(\frac{1}{\pi\, \omega}\right)^{\frac{1}{4}} e^{-\frac{p^2}{2\omega}} H_n\left(\frac{p}{\sqrt{\omega}}\right), \quad -\infty \le p \le \infty, \quad n = 0,1,\ldots. \tag{18}$$

The motivation behind this work is an examination of the Shannon entropies and mutual information sums in two-level superposition states. As one particular example, wave functions for a two-level system comprised of ground ($|00\rangle$) and excited ($|01\rangle$) states of two interacting oscillators can be written as

$$\Psi_{0001} = c_1|00\rangle + c_2|01\rangle\,, \tag{19}$$

here $|c_1|^2 + |c_2|^2 = 1$. The corresponding density matrix in this basis can be written as

$$\rho' = \begin{pmatrix} c_1^*\, c_1 & c_1^*\, c_2 \\ c_2^*\, c_1 & c_2^*\, c_2 \end{pmatrix}, \tag{20}$$

where the information about quantum interferences is contained in the off-diagonal terms. The c_1 and c_2 coefficients can be imaginary numbers but for simplicity we will restrict ourselves here to only consider real numbers. Hence, we fix the phase between the two coefficients at either zero or 180 degrees.

The superposition of states is a particular feature of quantum mechanics. We wish to examine how the entropic sums change in these states, with regard to the individual states comprising the superposition, and in relation to the uncertainty bound. Stronger uncertainty relation statements are related with values lying closer to the bound [75]. The bound exists due to the incompatibility of the position and momentum representations in quantum mechanics and is the best one can hope for. The entropy sum provides a quantitative measure of this incompatibility, and one can probe this for its dependence on the system parameters. From this perspective, it is a measure of the correlation between the position and momentum variables. If the one and two-variable (particle) entropy sums are measures of the position-momentum correlations, then the differences between them, the mutual information sum, should contain information about the influence of particle interaction on these correlations. Such arguments, based on consideration of Wigner functions, have been detailed [32,76].

One can ask how do these superposition states behave with regard to the entropic uncertainty relations, and how does this depend on the values of the coefficients? Furthermore, one can expect statistical correlations

J. Mex. Chem. Soc. **2024**, *68*(4)
Special Issue

ISSN-e 2594-0317

solely due to the superposition and quantum interferences that exist between the individual states. How are these additional correlations influenced by the interactions (attractive or repulsive) between the two particles? Hopefully, the ideas and results presented here will serve as a base to understand the effects of superposition which occur in other contexts, such as the behaviour of systems under the effects of external fields, or expansions in terms of multi-determinantal wave functions. In such cases, the physical description and information about these processes are mapped onto the coefficients.

Results and discussion

Harmonic oscillator

We begin the discussion by considering a two-level system of the harmonic oscillator comprised of the ground and first excited state. We wish to illustrate concepts here with one oscillator, that will aid in understanding the subsequent behaviour presented for two coupled oscillators. The wave function in position space is

$$\Psi_{01}(x) = c_1\psi_0(x) + c_2\psi_1(x), \tag{21}$$

and the integrals defining the information measures were evaluated numerically**.**

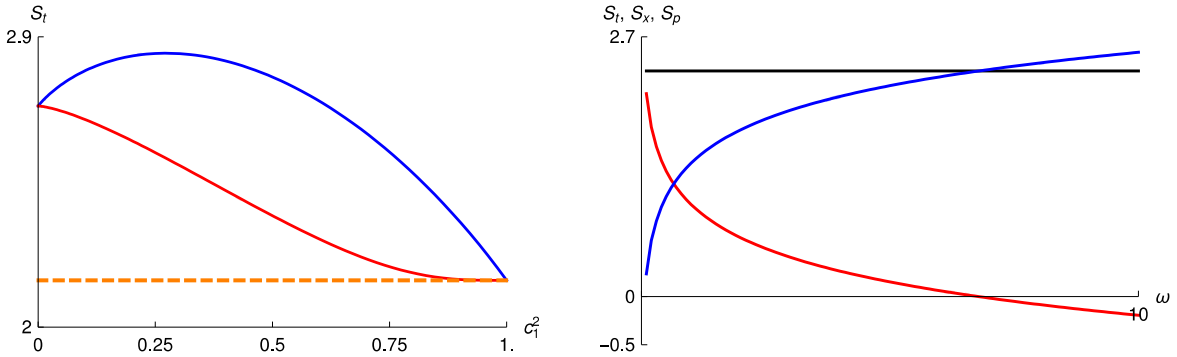

Fig. 1. Left: Plots of the entropic sum S_t of the Ψ_{01} superposition states with (red curve) and without (blue curve) quantum interferences varying c_1^2. The value of ω is set at unity and the horizontal dashed line is the $1 + \ln \pi$ bound. Right: Plots of the entropic sum S_t (black curve) and its position (red curve) and momentum (blue curve) components vs. ω for the Ψ_{01} superposition state with $c_1 = c_2 = 1/\sqrt{2}$.

The Shannon entropy sum as a function of c_1^2 is presented in Fig. 1. When $c_1^2 = 0$, the system is in the first excited state, while when $c_1^2 = 1$, it is in the ground state. One observes that the entropy sum decreases monotonically with c_1^2, until it saturates the uncertainty bound which is given by the dashed horizontal line. This concurs with the result that the uncertainty bound is saturated with the harmonic oscillator in its ground state [7,77]. Moreover, the entropy sum decreases from the first excited state to the ground state. This is in agreement with the result that the entropy sum increases with quantum number [7].

One can also examine the effects of the quantum interferences by eliminating them from the expression for the densities. This is achieved by suppressing the resulting c_1c_2 cross terms in the expressions for the densities. Fig. 1 illustrates that elimination of the quantum interferences moves the system further away from the uncertainty bound. On the other hand, the behaviour of the entropy sum, with and without quantum interferences, is distinct. The observed non-monotonic behaviour when no interferences are present, illustrate that there must be systems with different coefficients whose entropy sums are equal in value.

Studies of the ground and excited states of the harmonic oscillator have shown that their entropy sums are constant-valued as a function of ω, due to scaling of the wave function. This also holds for hydrogenic

J. Mex. Chem. Soc. **2024**, *68*(4)
Special Issue

ISSN-e 2594-0317

atoms when the nuclear charge is increased [7]. The right-hand side of Fig. 1 presents the behaviour of the entropy sum and its components for a superposition state, when ω is varied. The position space Shannon entropy decreases (localization), while the momentum space entropy increases (delocalization). The entropy sum here is also constant valued and lies above the uncertainty bound.

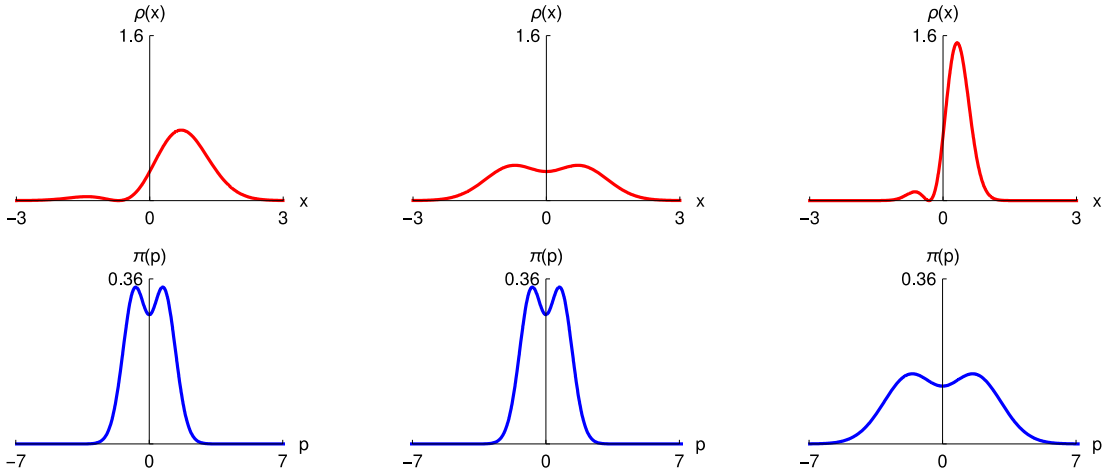

Fig. 2. Left column: Position and momentum space densities for the superposition state with $c_1 = c_2 = \frac{1}{\sqrt{2}}$ and $\omega = 1$. Middle column: Position and momentum space densities for the superposition state with $c_1 = c_2 = \frac{1}{\sqrt{2}}$ and $\omega = 1$ and no quantum interferences. Right column: Position and momentum space densities for the superposition state with $c_1 = c_2 = \frac{1}{\sqrt{2}}$ and $\omega = 5$.

The observed behaviours in Fig. 1 can be further analysed by examining the underlying position and momentum space distributions. These are presented in Fig. 2. The effects on the densities from (addition) removal of the quantum interferences can be seen by comparing the left and middle columns. These interferences induce a localization of the position space density toward the positive x regions. That the localization occurs in the positive x regions depends on the particular choice of coefficients. For example, the localization occurs in the negative x regions when c_2 is negative-valued.

On the other hand, there are no observed effects on the momentum space densities, which are equal. It is important to emphasize that this effect in momentum space, is a result of the different parities of the states used to construct the superposition, and the properties of the Fourier transform. The even parity ground state when Fourier transformed is real-valued while the odd parity first excited state is imaginary. Hence, there are no quantum interferences in momentum space, since these cancel when the density is constructed by multiplying the wave function by its complex conjugate. Thus, the differences in behaviour between entropy sums with and without quantum interferences, is due to position space. There is no cancellation if the states are of the same parity, and we shall return to this point in the last section.

Comparison of the left and right columns of Fig. 2 illustrates that larger ω localizes the position space density, while it delocalizes the density in momentum space. This is consistent with the behaviours of S_x and S_p presented in Fig. 1. The localization induced in the position space density from increasing ω, must be of an equal magnitude to the delocalization that the momentum density experiences. This is the reason why S_t is constant valued with ω.

Coupled oscillators

We now move on to analyse the behaviour when two oscillators interact either in an attractive or repulsive manner. Here, we will examine how the Shannon pair entropy sums, reduced entropy sums, and

J. Mex. Chem. Soc. **2024**, *68*(4)
Special Issue

ISSN-e 2594-0317

mutual information sums behave as c_1^2 is varied, and also as the intensity of the attractive or repulsive interaction potential is increased. The two superposition states that we will consider are symmetric (Ψ_{0001}) and antisymmetric (Ψ_{0111}) with respect to particle exchange. The last section is devoted to discussion of the Ψ_{0020} symmetric state which is of even parity.

Symmetric state

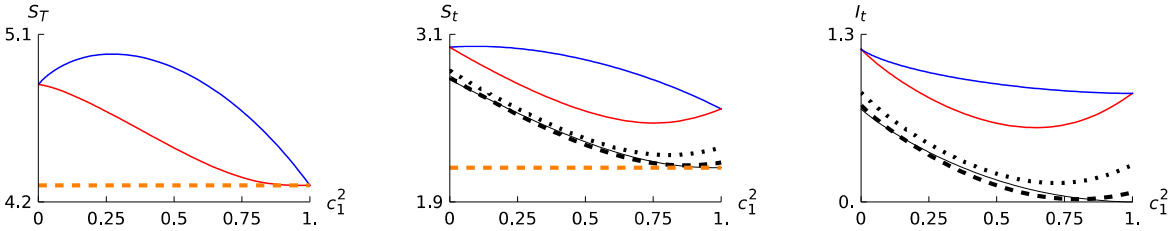

Fig. 3. Left: Plots of the Shannon pair entropic sum, S_T *vs* c_1^2 for the superposition function Ψ_{0010}, with attractive potential (λ = 5), with (red curve) and without (blue curve) quantum interferences. The horizontal dashed line is the 2(1 + ln π) uncertainty bound. Center: Plots of the reduced entropic sum S_t from the superposition function (λ = 5) with (red curve) and without (blue curve) quantum interferences. The curves in black correspond to the superposition state with different values of λ (0-solid,1-dashed, 2-dotted). The horizontal dashed line is the 1 + ln π bound. Right: Plots of the information sum I_t *vs* c_1^2 for the superposition function (λ = 5) with (red curve) and without (blue curve) quantum interferences. Curves in black are as previously defined. The value of ω is set at unity in all curves.

The Shannon pair entropy sums are presented in Fig. 3. These results are similar to the ones in Fig. 1 for S_t of the single oscillator. S_T saturates the uncertainty bound for the ground state system when $c_1^2 = 1$, and increases as c_1^2 decreases, as the state moves towards the first excited one. One characteristic of these two-particle systems is that their S_T values are independent of the interaction strength (λ). Thus the curves which are presented are representative for all values of λ. The interpretation upon comparison of the curves with and without quantum interferences, is that the interferences move the S_T values closer to the bound.

This is also consistent with the curves for S_t presented in the center plot, with some important differences. First, the reduced entropy sum, S_t, does depend on λ. Different curves in black, corresponding to different λ values, are now presented. We ask the reader to consider the solid line for the non-interacting system with λ = 0. The curve when λ = 2 (dotted) is above the non-interacting one, which shows that interactions increase S_t, with movement away from the bound. This occurs for all values of c_1^2.

On the other hand, one can observe that there is a region of c_1^2 values where the curve for relatively weaker interactions with λ = 1 (dashed line), lies below the non-interacting one. This effect is due to the superposition, since all interacting values are above those of the constituent states at $c_1^2 = 0$, and at $c_1^2 = 1$. Furthermore, the presence of minima in the S_t curves when interaction is included can be attributed to these interactions. Note that the non-interacting curve does not present a minimum. As c_1^2 approaches unity, the interacting systems move away from the bound which results in the minima. Even the curve for λ = 1, which is below the non-interacting curve at smaller c_1^2, is now above it as c_1^2 approaches unity.

Inspection of the curves for the mutual information sums shows that the curve corresponding to no quantum interferences, lies above the one with the interferences present. In general, the correlation is larger with increasing λ. However, similar to S_t, there is a region where the λ = 1 curve dips below the non-interacting one. Thus, superposition in an interacting system can result in a correlation that is smaller than the corresponding non-interacting case, when in the presence of an attractive potential. One can also observe that the relative orderings at $c_1^2 = 0{,}1$ are as expected. That is, the mutual information sums increase with increasing λ.

These tendencies can be further probed by examining how I_t changes with λ for different values of c_1^2. The curves presented in Fig. 4 illustrate that I_t presents minima at the chosen values of c_1^2. Thus, there are

J. Mex. Chem. Soc. **2024**, *68*(4)
Special Issue

ISSN-e 2594-0317

regions where increasing the intensity of interactions yields a smaller correlation, opposite to the increasing general tendency, present in the larger λ regions. These minima are due to the S_t component as shown in the row below, since S_T is constant valued with λ.

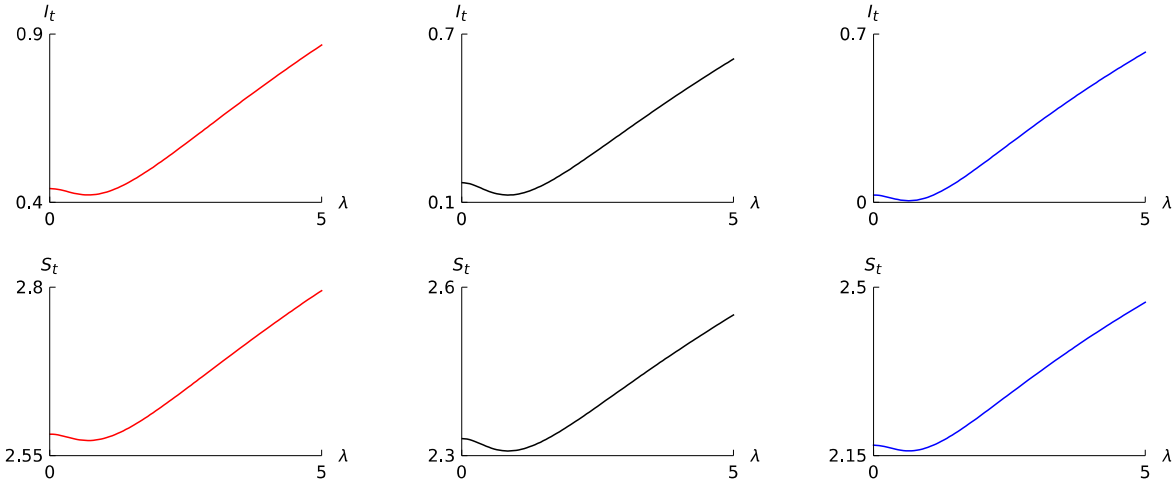

Fig. 4. First row: Plots of the mutual information sum, I_t vs. λ from the superposition function Ψ_{0010}, with attractive potential. Left: ($c_1^2 = 0.2$) Middle: ($c_1^2 = 0.5$) Right: ($c_1^2 = 0.8$). Second row: Plots of S_t for the systems in the row above. The value of ω is set at unity in all curves.

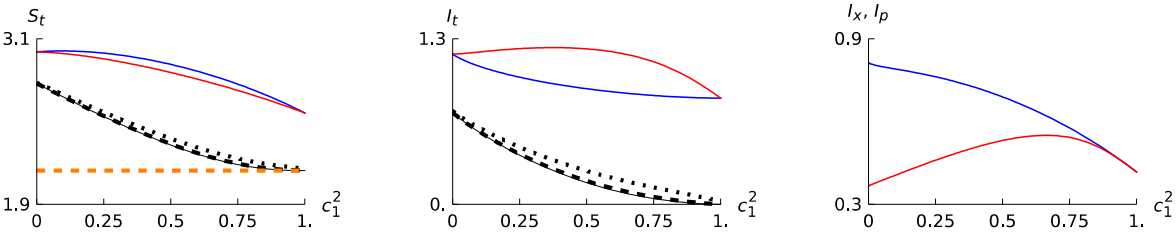

Fig. 5. Left: Plots of the reduced entropic sum, S_t, from the superposition function Ψ_{0010}, with repulsive potential (λ = 0.7), with (red curve) and without (blue curve) quantum interferences. The curves in black correspond to the superposition state with different values of λ (0-solid, 0.25-dashed, 0.5-dotted). The horizontal dashed line is the 1+ln π bound. Center: Plots of the information sum I_t vs. c_1^2 for the superposition function (λ = 0.7) with (red curve) and without (blue curve) quantum interferences. Curves in black are as previously defined. Right: Plots of the I_x (red curve) and I_p (blue curve) components with λ = 0.7 vs. c_1^2. The value of ω is set at unity in all curves.

We now focus our attention on the results for the repulsive potential in Fig. 5. The corresponding curves for S_T are not presented here, since they are exactly the same as the ones for the attractive potential in Fig. 3, as the S_T values do not depend on the value or nature of the potential. The results in the relative ordering of the S_t curves with and without quantum interferences, is consistent with those from Fig. 3 for the attractive potential. That is, the quantum interferences move the values closer to the uncertainty bound. However, one can see that this effect is smaller for the repulsive case as compared to the attractive one. It is also noteworthy that all different λ-valued curves are bounded by the non-interacting one, and these are ordered with the particular λ value. Increased interaction thus induces a movement of S_t away from the uncertainty bound, for all c_1^2 values. This is distinct from the attractive case, where the λ = 1 curve was observed to be lower than the non-interacting one, in a region of c_1^2 values.

J. Mex. Chem. Soc. **2024**, *68*(4)
Special Issue

ISSN-e 2594-0317

Examination of the $\lambda = 0.7$ curves for the mutual information sum show that the correlation is now larger when the quantum interferences are included. This is different from the attractive case (Fig. 3), where the opposite is observed. Furthermore, all the different λ-valued curves are lower bounded by the non-interacting curve. The I_t curves increase in value away from the non-interacting one as λ increases. Again, this is distinct from the attractive case. The I_x and I_p components are also presented. In contrast to I_p, I_x presents a minimum. While $I_p > I_x$ at smaller c_1^2, the two components approach each other in value at larger c_1^2, and are equal when $c_1^2 = 1$.

Antisymmetric state

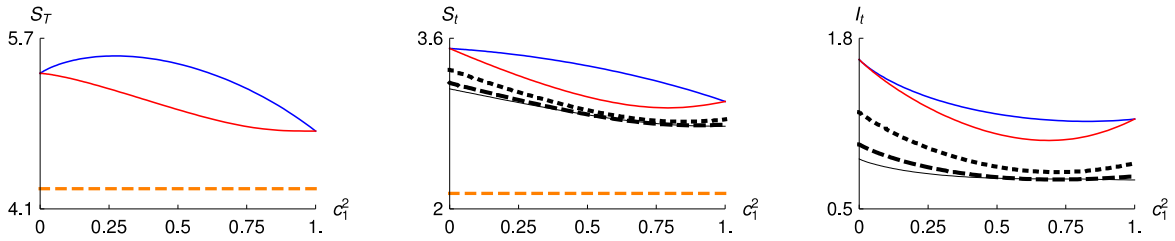

Fig. 6. Left: Plots of the Shannon pair entropic sum, S_T vs c_1^2 for the superposition function Ψ_{0111}, with attractive potential ($\lambda = 5$), with (red curve) and without (blue curve) quantum interferences. The horizontal dashed line is the $2(1 + \ln \pi)$ uncertainty bound. Center: Plots of the reduced entropic sum S_t from the superposition function ($\lambda = 5$) with (red curve) and without (blue curve) quantum interferences. The curves in black correspond to the superposition state with different values of λ (0-solid, 1-dashed, 2-dotted). The horizontal dashed line is the $1 + \ln \pi$ bound. Right: Plots of the information sum I_t vs. c_1^2 for the superposition function ($\lambda = 5$) with (red curve) and without (blue curve) quantum interferences. Curves in black are as previously defined. The value of ω is set at unity in all curves.

The plots for the antisymmetric state with attractive potential are presented in Fig. 6. The results are consistent with those presented and discussed for the symmetric state. There are, however, some notable differences in the curves for S_t and I_t. In general, the curves are ordered with respect to their λ-values. Moreover, it seems that the region where the $\lambda = 1$ curve dips below the non-interacting ($\lambda = 0$) one, is smaller for this antisymmetric state as compared to the symmetric one (Fig. 3). This effect is not as pronounced here as was seen for the symmetric state, and thus suggests that this could be due to wave function symmetry.

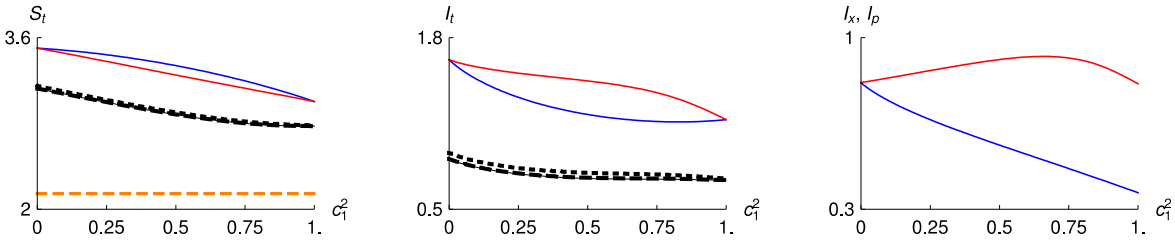

Fig. 7: Left: Plots of the reduced entropic sum, S_t, from the superposition function Ψ_{0111}, with repulsive potential ($\lambda = 0.7$), with (red curve) and without (blue curve) quantum interferences. The curves in black correspond to the superposition state with different values of λ (0-solid, 0.25-dashed, 0.5-dotted). The horizontal dashed line is the $1+\ln \pi$ bound. Center: Plots of the information sum I_t vs. c_1^2 for the superposition function ($\lambda = 0.7$) with (red curve) and without (blue curve) quantum interferences. Curves in black are as previously defined. Right: Plots of the I_x (red curve) and I_p (blue curve) components with $\lambda = 0.7$ vs. c_1^2. The value of ω is set at unity in all curves.

J. Mex. Chem. Soc. **2024**, *68*(4)
Special Issue

ISSN-e 2594-0317

Fig. 7 presents the results for the antisymmetric state in the presence of repulsive potentials. The curves are again consistent with those for the symmetric state. However, now $I_x > I_p$, which is opposite to that observed in the symmetric state.

Same-parity superposition state

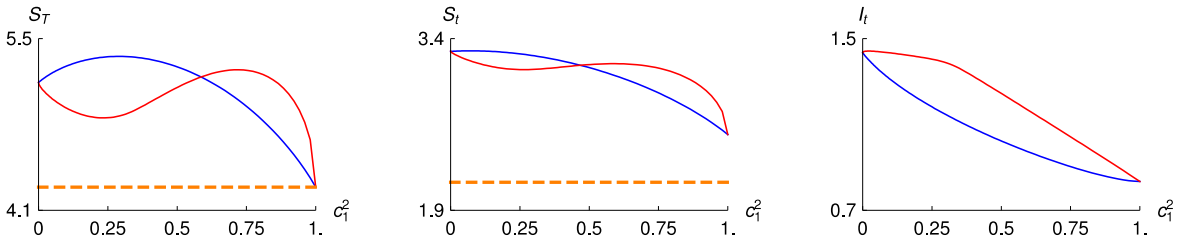

Fig. 8. Left: Plots of the Shannon pair entropic sum, S_T, vs. c_1^2 for the superposition function Ψ_{0020}, with repulsive potential (λ = 0.7), with (red curve) and without (blue curve) quantum interferences. The horizontal dashed line is the 2(1 + ln π) uncertainty bound. Center: Plots of the reduced entropic sum S_t from the superposition function (λ = 0.7) with (red curve) and without (blue curve) quantum interferences. The horizontal dashed line is the 1 + ln π bound. Right: Plots of the information sum I_t vs. c_1^2 for the superposition function (λ = 0.7) with (red curve) and without (blue curve) quantum interferences. The value of ω is set at unity in all curves.

Results are presented here for a symmetric superposition state Ψ_{0020} with components $|00\rangle$ and $|20\rangle$, in the presence of a repulsive potential. There are now two additional effects that are present here. The first is that the second component is a more highly excited state. The second is the even-function parity of both components, which results in quantum interferences being present in momentum space.

Fig. 8 illustrates that these effects provoke differences from the previous results. First, the result that S_T and S_t are closer to the respective bound when quantum interferences are present, is only valid for particular (smaller) values of c_1^2. At larger values, the curves invert, and it is the curve without quantum interferences that is closest to the bound. This crossover between regimes occurs at $c_1 = c_2 = 1/\sqrt{2}$ for S_t, while it is shifted to the right in the S_T crossover.

The behaviour of the mutual information sum is consistent for the other states with repulsive potentials. That is, the correlation is larger with quantum interferences. There is another difference in the case of attractive potentials (λ = 5), which is not presented here for brevity. The curve with the quantum interferences now lies above the one without the interferences. This is similar to the result for the repulsive potential, and different from the previous ones presented for attractive potentials. Analysis of different λ values is not presented here since the resulting curves are very close together. These results highlight the importance of additional effects when higher excited states and parities are taken into consideration.

Conclusions

The effects of superposition on the entropic uncertainty relations and mutual information sums, are examined in two-level superposition states of two coupled oscillators. The changes in behaviour with the presence of an attractive or repulsive interaction potential, and the interaction strength, are explored. We find that the inclusion of quantum interferences generated by the superposition, leads to a movement of the entropy sums toward the respective uncertainty bound, when compared to the respective states with no quantum interferences. This is observed in the presence of both attractive and repulsive inter-particle potentials. However, there are notable differences when examining the correlation sums. The presence of quantum interferences augments the correlation in the presence of a repulsive potential, while it suppresses the correlation

J. Mex. Chem. Soc. **2024**, *68*(4)
Special Issue

ISSN-e 2594-0317

when an attractive potential is present. We also observe that superposition in the presence of attractive potentials, is able to generate states which are lesser correlated than the corresponding non-interacting ones. On the other hand, this is not observed for the repulsive potential, where all values are lower bounded by the corresponding non-interacting ones. The regions where the interacting states with attractive potentials are lesser correlated than the non-interacting ones, are observed to be smaller when the state is antisymmetric. The role of function parity and excitation in the superposition state, and their effects on the information measures, are discussed.

References

1. Robertson, H. *P. Phys. Rev.* **1929**, *34*, 163. DOI: https://doi.org/10.1103/PhysRev.34.163.
2. Zewail, A. H. *J. Phys. Chem. A* **2000**, *104*, 5660. DOI: https://doi.org/10.1021/jp001460h.
3. Beckner, W. *Ann. Math.* **1975**, *102*, 159–182. DOI: https://doi.org/10.2307/1970980.
4. Bialynicki-Birula, I.; Mycielski, J. *Commun.Math. Phys.* **1975**, *44*, 129–132. DOI: https://doi.org/10.1007/BF01608825.
5. Hertz, A.; Cerf, N. J. *J. Phys. A: Math. Theor.* **2019**, *52*, 173001. DOI: https://doi.org/10.1088/1751-8121/ab03f3.
6. Yáñez, R. J.; van Assche, W.; Dehesa, J. S. *Phys. Rev. A* **1994**, *50*, 3065. DOI: https://doi.org/10.1103/PhysRevA.50.3065.
7. Gadre, S. R.; Sears, S. B.; Chakravorty, S. J.; Bendale, R. D. *Phys. Rev. A* **1985**, *32*, 2602. DOI: https://doi.org/10.1103/PhysRevA.32.2602.
8. Maasen, S. E.; Panos, C. P. *Phys. Lett. A.* **1998**, *246*, 530. DOI: https://doi.org/10.1016/S0375-9601(98)00524-6.
9. Grassi, A.; Lombardo, G. M.; March, N. H.; Pucci, R. *Int. J. Quantum Chem.* **1998**, *69*, 721–726. DOI: https://doi.org/10.1002/(SICI)1097-461X(1998)69:6<721::AID-QUA4>3.0.CO;2-X.
10. Guevara, N. L.; Sagar, R. P.; Esquivel, R. O. *Phys. Rev. A* **2003**, *67*, 012507. DOI: https://doi.org/10.1103/PhysRevA.67.012507.
11. Romera, E.; Dehesa, J. S. *J. Chem. Phys.* **2004**, *120*, 8906–8912. DOI: https://doi.org/10.1063/1.1697374.
12. Shi, Q.; Kais, S. *J. Chem. Phys.* **2004**, *121*, 5611–5617. DOI: https://doi.org/10.1063/1.1785773.
13. Chatzisavvas, K. C.; Moustakidis, C. C.; Panos, C. P. *J. Chem. Phys.* **2005**, *123*, 174111. DOI: https://doi.org/10.1063/1.2121610.
14. Sen, K.; Katriel, J. *J. Chem. Phys.* **2006**, *125*, 074117. DOI: https://doi.org/10.1063/1.2263710.
15. Nagy, Á. *Int. J. Quantum Chem.* **2014**, *115*, 1392–1395. DOI: https://doi.org/10.1002/qua.24812.
16. Lin, C. H.; Ho, Y. K. *Chem. Phys. Lett.* **2015**, *633*, 261–264. DOI: https://doi.org/10.1016/j.cplett.2015.05.029.
17. Pooja; Kumar, R.; Kumar, G.; Kumar, R.; Kumar, A. *Int. J. Quantum Chem.* **2016**, *116*, 1413. DOI: https://doi.org/10.1002/qua.25197.
18. Coles, P. J.; Berta, M.; Tomamichel, M.; Wehner, S. *Rev. Mod. Phys.* **2017**, *89*, 015002. DOI: https://doi.org/10.1103/RevModPhys.89.015002.
19. Sekh, G. A.; Saha, A.; Talukdar, B. *Phys. Lett. A* **2018**, *382*, 315. DOI: https://doi.org/10.1016/j.physleta.2017.12.005.
20. Flores-Gallegos, N. *Chem. Phys. Lett.* **2019**, *720*, 1–6. DOI: https://doi.org/10.1016/j.cplett.2019.01.049.
21. Kumar, R. K.; Chakrabarti, B.; Gammal, A. *J. Low Temp. Phys.* **2019**, *194*, 14. DOI: https://doi.org/10.1007/s10909-018-2051-8.
22. Zhao, Q.; Zhao, J. *J. Low Temp. Phys.* **2019**, *194*, 302. DOI: https://doi.org/10.1007/s10909-018-2099-5.
23. Panos, C. P.; Moustakidis, C. C. *Physica A: Stat. Mech. Appl.* **2019**, *518*, 384. DOI: https://doi.org/10.1016/j.physa.2018.12.018.
24. Nasser, I.; Zeama, M.; Abdel-Hady A. *Int. J. Quan. Chem.*, *121*:e26499, **2021**. DOI: https://doi.org/10.1002/qua.26499.

J. Mex. Chem. Soc. **2024**, *68*(4)
Special Issue

ISSN-e 2594-0317

25. (a)Ho, M.; Smith Jr., V.; Weaver, D.; Gatti, C.; Sagar, R.; Esquivel, R. *J. Chem. Phys.* **1998**, *108*, 5469. DOI: https://doi.org/10.1063/1.476316. (b) Ho, M.; Weaver, D.; Smith Jr., V.; Sagar, R.; Esquivel, R.; Yamamoto, S. *J. Chem. Phys.* **1998**, *109*, 10620. DOI: https://doi.org/10.1063/1.477761.
26. Liu, S. *J. Chem. Phys.* **2007**, *126*, 191107. DOI: https://doi.org/10.1063/1.2741244.
27. Ho, M.; Weaver, D.; Smith Jr., V.; Sagar, R.; Esquivel, R. *Phys. Rev. A.* **1998**, *57*, 4512. DOI: https://doi.org/10.1103/PhysRevA.57.4512.
28. Thakkar, A. J. John Wiley & Sons, Ltd, 2003; Chapter 5, pp 303–352. DOI: https://doi.org/10.1002/0471484237.ch5.
29. Dunkel, J.; Trigger, S. A. *Phys. Rev. A* **2005**, *71*, 052102. DOI: https://doi.org/10.1103/PhysRevA.71.052102.
30. Garbaczewski, P. *Phys. Rev. A* **2005**, *72*, 056101. DOI: https://doi.org/10.1103/PhysRevA.72.056101.
31. Laguna, H. G.; Sagar, R. P. *Int. J. Quant. Inf.* **2010**, *08*, 1089–1100. DOI: https://doi.org/10.1142/S0219749910006484.
32. Salazar, S. J. C.; Laguna, H. G.; Sagar, R. P. *Phys. Rev. A* **2023**, *107*, 042417. DOI: https://doi.org/10.1103/PhysRevA.107.042417.
33. Mukherjee, N.; Roy, A. K. *Int. J. Quantum Chem.* **2018**, *118*, e25596. DOI: https://doi.org/10.1002/qua.25596.
34. Majumdar, S.; Roy, A. *Quantum Rep.* **2020**, *2*, 189. DOI: https://doi.org/10.3390/quantum2010012.
35. Estañón, C. R.; Aquino, N.; Puertas-Centeno, D.; Dehesa, J. S. *Int. J. Quantum Chem.* **2020**, *120*, e26192. DOI: https://doi.org/10.1002/qua.26192.
36. Salazar, S. J. C.; Laguna, H.; Prasad, V.; Sagar, R. P. *Int J Quant Chem* **2020**, *120*, e26188. DOI: https://doi.org/10.1002/qua.26188.
37. Olendski, O. *Entropy* **2019**, *21*, 1060. DOI: https://doi.org/10.3390/e21111060.
38. Sen, K. D. *J. Chem. Phys.* **2005**, *123*, 074110. DOI: https://doi.org/10.1063/1.2008212.
39. Nascimento, W. S.; Prudente, F. V. *Chem. Phys. Lett.* **2018**, *691*, 401. DOI: https://doi.org/10.1016/j.cplett.2017.11.048.
40. Aquino, N.; Flores-Riveros, A.; Rivas-Silva, J. F. *Phys. Lett. A* **2013**, *377*, 2062. DOI: https://doi.org/10.1016/j.physleta.2013.05.048.
41. Martínez-Sánchez, M. A.; Vargas, R.; Garza, J. *Quantum Reports* **2019**, *1*, 208–218. DOI: https://doi.org/10.3390/quantum1020018.
42. Fotue, A. J.; Kenfack, S. C.; Tiotsup, M.; Issofa, N.; Wirngo, A. V.; Djemmo, M. P. T.; Fotsin, H.; Fai, L. C. *Mod. Phys. Lett.* B **2015**, *29*, 1550241. DOI: https://doi.org/10.1142/S0217984915502413.
43. Ghosal, A.; Mukherjee, N.; Roy, A. K. A*nn. Phys. (Berlin)* **2016**, *528*, 796. DOI: https://doi.org/10.1002/andp.201600121.
44. Mukerjee, N.; Roy, A. K. *Ann. Phys.* **2016**, *528*, 412–433. DOI: https://doi.org/10.1002/andp.201500301.
45. Nagy, Á. in Density Matrix and Density Functional Theory in Atoms, Molecules and the Solid State. Dordrecht, **2003**; pp 79–87.
46. Higuchi, M.; Higuchi, K. *Comp. Theo. Chem.* **2013**, *1003*, 91–96. DOI: https://doi.org/10.1016/j.comptc.2012.09.015.
47. Sharma, P.; Bao, J. J.; Truhlar, D. G.; Gagliardi, L. *Ann. Rev. Phys. Chem.* **2021**, *72*, 541–564. DOI: https://doi.org/10.1146/annurev-physchem-090419-043839.
48. Guevara, N. L.; Sagar, R. P.; Esquivel, R. O. *J. Chem. Phys.* **2003**, *119*, 7030. DOI: https://doi.org/10.1063/1.1605932.
49. Sagar, R. P.; Laguna, H. G.; Guevara, N. L. *Int. J. Quantum Chem.* **2011**, *111*, 3497. DOI: https://doi.org/10.1002/qua.22792.
50. López-Rosa, S.; Martín, A. L.; Antolín, J.; Angulo, J. C. *Int. J. Quantum Chem.* **2019**, *119*, e25861. DOI: https://doi.org/10.1002/qua.25861.
51. Laguna, H.; Sagar, R. *Phys. Rev. A* **2011**, *84*, 012502. DOI: https://doi.org/10.1103/PhysRevA.84.012502.
52. Salazar, S.; Laguna, H. G.; Sagar, R. P. *Phys. Rev.* A **2020**, *101*, 042105. DOI: https://doi.org/10.1103/PhysRevA.101.042105, and references therein.

J. Mex. Chem. Soc. **2024**, *68*(4)
Special Issue

ISSN-e 2594-0317

53. Löwdin, P.-O. *Phys. Rev.* **1955**, *97*, 1509. DOI: https://doi.org/10.1103/PhysRev.97.1509.
54. Wigner, E.; Seitz, F. *Phys. Rev.* **1933**, *43*, 804–810. DOI: https://doi.org/10.1103/PhysRev.43.804.
55. Kutzelnigg, W.; Re, G. D.; Berthier, G. *Phys. Rev.* **1968**, *172*, 49. DOI: https://doi.org/10.1103/PhysRev.172.49.
56. Thakkar, A. J.; Smith Jr., V. H. *Phys. Rev. A* **1981**, *23*, 473. DOI: https://doi.org/10.1103/PhysRevA.23.473.
57. Park, D. *Quantum Inf. Process.* **2020**, *19*, 129. DOI: https://doi.org/10.1007/s11128-020-02626-4.
58. Faba, J.; Martín, V.; Robledo, L. *Phys. Rev. A* **2021**, *104*, 032428. DOI: https://doi.org/10.1103/PhysRevA.104.032428.
59. Tam, P. M.; Claassen, M.; Kane, C. L. *Phys. Rev. X* **2022**, *12*, 031022. DOI: https://doi.org/10.1103/PhysRevX.12.031022.
60. Angulo, J. C.; López-Rosa, S. *Entropy* **2022**, *24*, 233. DOI: https://doi.org/10.3390/e24020233.
61. Schürger, P.; Engel, V. *Phys. Chem. Chem. Phys.* **2023**, *25*, 28373. DOI: https://doi.org/10.1039/d3cp03573e.
62. Alonso-López, D.; Cembranos, J. A. R.; Díaz-Guerra, D.; Mínguez-Sánchez, A. *Eur. Phys. J. D* **2023**, *77*, 43. DOI: https://doi.org/10.1140/ep jd/s10053-023-00629-1.
63. Schürger, P.; Engel, V. AIP Advances **2023**, 13, 125307. DOI: https://doi.org/10.1063/5.0180004.
64. Kumar, K.; Prasad, V. A*nn. Phys. (Berlin)* **2023**, *535*, 2300166. DOI: https://doi.org/10.1002/andp.202300166.
65. Peng, H. T.; Ho, Y. K. *Entropy* **2015**, *17*, 1882–1895. DOI: https://doi.org/10.3390/e17041882.
66. Sagar, R. P.; Guevara, N. L. *J. Chem. Phys.* **2005**, *123*, 044108. DOI: https://doi.org/10.1063/1.1953327.
67. Moshinsky, M. *Am. J. Phys.* **1968**, *36*, 52–53. DOI: https://doi.org/10.1119/1.1974410.
68. Holas, A.; Howard, I.; March, N. *Phys. Lett. A* **2003**, *310*, 451–456. DOI: https://doi.org/10.1016/S0375-9601(03)00408-0.
69. Ragot, S. *J. Chem. Phys.* **2006**, *125*, 014106. DOI: https://doi.org/10.1063/1.2212935.
70. March, N. H.; Cabo, A.; Claro, F.; Angilella, G. G. N. Phys. Rev. A 2008, 77, 042504. DOI: https://doi.org/10.1103/PhysRevA.77.042504.
71. Dahl, J. P. Can. J. Chem. 2009, 87, 784–789. DOI: https://doi.org/10.1139/V09-002.
72. Niehaus, T.; March, N. Theor. Chem. Acc. 2010, 125, 427. DOI: https://doi.org/10.1007/s00214-009-0578-0.
73. Benavides-Riveros, C.; Várilly, J. Eur. Phys. J. D 2012, 66, 274. DOI: https://doi.org/10.1140/epjd/e2012-30442-4.
74. Ebrahimi-Fard, K.; Gracia-Bondía, J. J. Math. Chem. 2012, 50, 440. DOI: https://doi.org/10.1007/s10910-011-9822-7.
75. Floerchinger, S.; Haas, T.; Müller-Groeling, H. Phys. Rev. A. 2021, 103, 062222. DOI: https://doi.org/10.1103/PhysRevA.103.062222.
76. Laguna, H.; Sagar, R. J. Phys. A: Math. Theor. 2012, 45, 025307. DOI: https://doi.org/10.1088/1751-8113/45/2/025307.
77. Majerník, V.; Opatrny, T. J. Phys. A: Math Gen. 1996, 29, 2187. DOI: https://doi.org/10.1088/0305-4470/29/9/029.